Clustering Fluctuation Patterns of Groundwater Levels in Tokyo Caused by the Great East Japan Earthquake Using Self-Organizing Maps

Akira KAWAMURA[1, *], Shigeyuki ISHIHARA[2], Hideo AMAGUCHI[1] and Tadakatsu TAKASAKI[2]

[1] Graduate School of Urban Environmental Engineering, Tokyo Metropolitan University, 1-1 Minami-Ohsawa, Hachioji, Tokyo 192-0397, Japan
[2] Bureau of Construction, Tokyo Metropolitan Government, 2-8-1 Nishi-Shinjyuku, Shinjyuku, Tokyo 163-8001, Japan
[*] e-mail: kawamura@tmu.ac.jp phone: +81-42-677-2787

Abstract: The Great East Japan Earthquake occurred at 14:46 JST on March 11, 2011, which was the strongest earthquake on record in Japan. When the earthquake occurred, large fluctuations of groundwater levels were observed at 102 observation wells in Tokyo, although Tokyo is located around 400 km away from the epicenter. In this study, we investigate and cluster the fluctuation patterns of hourly groundwater levels using self-organizing maps. As for the results, the fluctuation patterns of the groundwater level were classified into eight clusters. Spacio-temporal characteristics of these patterns including their causes were investigated in detail.

1 INTRODUCTION

Whole Japanese Archipelago and Southeast Asian region are in serious peril of severe earthquakes, because it is situated in the Circum-Pacific Seismic Zone. Most of the megacities not only in Japan but also Southeast Asian countries are located on the alluvial plains where the ground is very soft and especially vulnerable for groundwater related disasters like landslides and liquefactions.

A earthquake of 5 upper intensity was observed in the Tokyo Metropolitan area due to the 9.0 moment magnitude (Mw) 2011 off the Pacific coast of Tohoku earthquake (hereafter called “the Great East Japan Earthquake”), which occurred at 2:46 JST on 11 March 2011, off the coast of Sanriku in the northeastern part of the Japanese mainland. Many aftershocks and post-seismic slips, such as the intensity of 5 lower (Mw 7.4) earthquake which occurred at 3:15 p.m. on the same day, triggered some phenomena including liquefaction and unique fluctuation of groundwater levels (JMA, 2012; AIST-GSJ, 2011, Itadera et al., 2011; Kawai et al., 2012).

It is very important to understand this change caused by the earthquake correctly, not only for developing countermeasures for land subsidence and liquefaction, but also for water resource management. In addition, evaluating the rapid change of groundwater level after the earthquake is effective to predict its influence on hydrologic cycle, and it will be valuable for future research.

Regarding the relationship between groundwater and the Great East Japan Earthquake observed by the Active Fault and Earthquake Research Center, the National Institute of Advanced Industrial Science and Technology, Kitagawa et al. (2011) reported on changes of the groundwater level, groundwater pressure, and the amount of artesian water flow in the day after the earthquake in the areas of Tokai, Kinki and Shikoku. Although some phenomena such as the rising or lowering of groundwater level, and the increased amount and rising temperature of hot spring water were observed all over Japan after the Great East Japan Earthquake, no detailed analyses can be found on the change before and after the earthquake (Kagawa et al., 2013; Itadera et al., 2011). Most of the past research and studies on the groundwater in the Tokyo area can be classified into the following categories: reports on the groundwater itself (kokubun and Tsuchiya, 2003), reports on the relationship between groundwater and land subsidence (TMG-BE, 2011), and reports on the fluctuation of groundwater level based on predictions of earthquake precursors (TMG, 1979). Research and studies on fluctuations of unconfined and confined groundwater levels, however, do not appear to have been published.

Using hourly observation data for the month of the Great East Japan Earthquake (March 2011) which was collected from the groundwater level observation system in the Civil Engineering and Training Center (CETC) of Tokyo Metropolitan Government (TMG), the authors categorized the time-series behaviors of the groundwater fluctuation into seven confined and three unconfined groundwater level patterns by authors'visual inspections (Ishihara et al., 2012). However, data from observed records of groundwater level after the Great East Japan Earthquake is very rare, and is difficult to compare or verify. To analyze the characteristics of the unprecedented and complicated fluctuation of groundwater level, it is important to summarize the patterns using more objective analyses which do not rely on subjective classification. Self-Organizing Maps (SOMs) are a pattern classification technique, which have more advantages for finding data characteristics than other techniques, such as visualizing the interconnectedness of complicated data on two-dimensional surfaces (Kohonen, 1990). Therefore, SOMs are often used in the areas of hydrology (Iseri et al., 2010; Nishiyama et al., 2005; Iseri et al., 2013) and meteorology (Nguyen et al., 2015), however, they do not seem to have been used for categorizing the characteristics of groundwater level.

In this paper, therefore, the characteristics of confined and unconfined groundwater level are objectively evaluated with SOMs using hourly data captured by the observation system for groundwater level in CETC in the month of March 2011, when the Great East Japan Earthquake occurred. From a comparative review of these results and those of subjective classifications based on the time-series behaviors described earlier, more specific fluctuation patterns and classification characteristics become clear.

2 MATERIALS AND METHODS

2.1 Overview of the groundwater level observation system in the Tokyo Metropolis

Figure 1 shows the location of Tokyo, and Figure 2 shows the locations and numbers of the groundwater level observation sites in the Tokyo Metropolitan area (TMG-CETC, 2012). The Tokyo Metropolitan area stretches from west to east with a mountainous district in the west, a central terrace called the Musashino Plateau, and eastern lowlands bordering Tokyo Bay. Tokyo Metropolis covers an area of about 1,580 km^2 (excluding the islands and mountains of Tokyo).

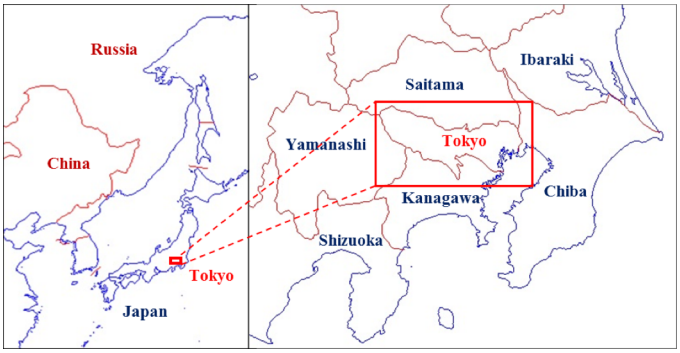

Figure 1. Tokyo location map

2.2 Data used

Using hourly observation data for the month of the Great East

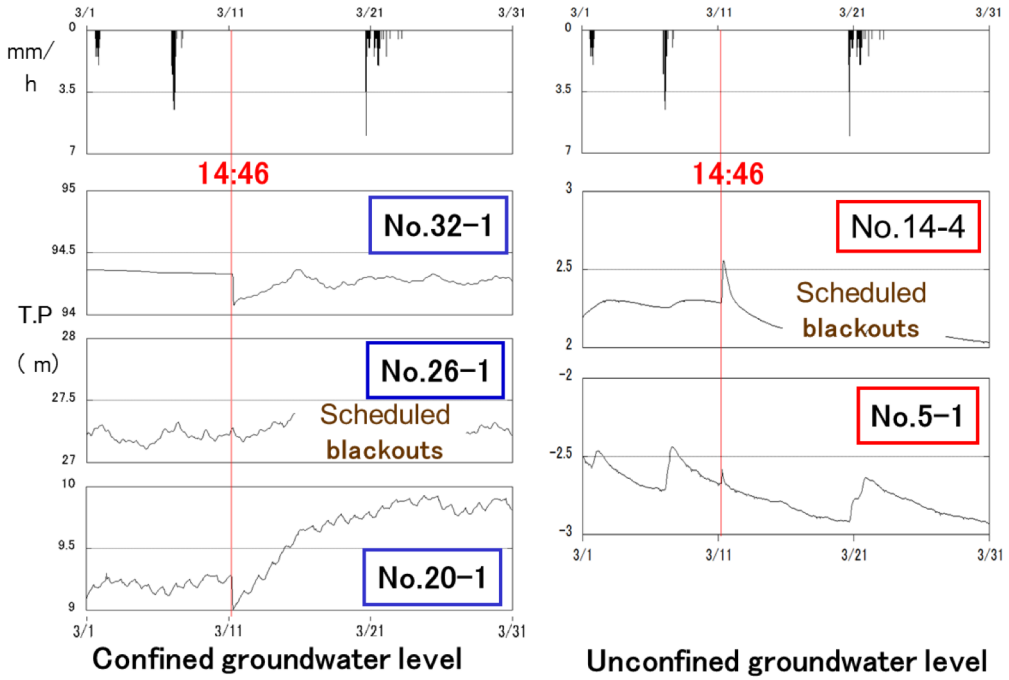

Figure 3. Time-series behaviors of the groundwater level fluctuation

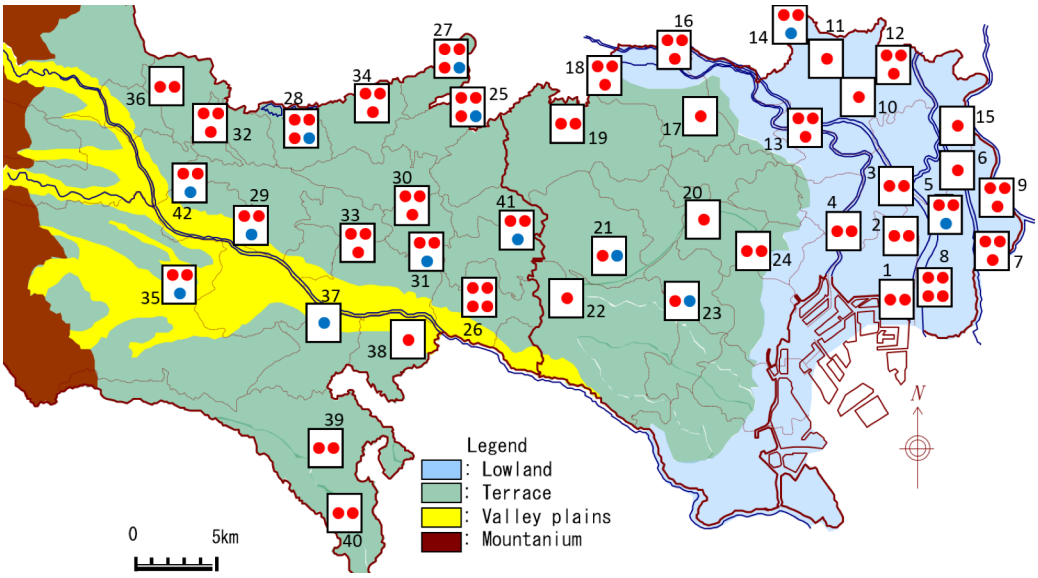

Figure 2. Location of groundwater level observation sites

Japan Earthquake which was collected from the groundwater level observation system in the Civil Engineering and Training Center, the authors investigated the time-series behaviors of the groundwater level fluctuation and found that the earthquake caused changes as shown in Fig. 3.

Some data are missing in March 2011 due to Tokyo Electric Power Co. Inc.'s planned blackouts (TEPCO, 2011). Therefore, 5 items, (a) to (e) below, are used as input data from 98 wells (confined: 85, unconfined: 13) in 40 observation sites, where the data were less affected by the blackouts.

The SOM input data were standardized so that even a slight or long term water

level change could be extracted from the raw data shown in Table 1.

(a) The difference of water levels before and after the earthquake (cm) ; 16:00, 11 March – 14:00 of the same day.

(b) The difference of water levels immediately after the earthquake and 22 hours later (cm) ; 14:00, 12 March - 16:00, 11 March.

(c) The difference of water levels the day after the earthquake and two days later (cm) ; the mean value of 14 March - 14:00, 12 March.

(d) The long term difference of water levels two days after the earthquake and 31 March (cm) ; the mean value of 31 March – that of 14 March.

(e) The altitude value of the depth of the screen in each observation well. (T.P. : Tokyo Peil ; standard mean sea level of Tokyo Bay in Japan)

The reason that the depth of the strainers is included in the items above is to classify the confined and unconfined groundwater level accurately.

2.3 Application of Self-Organizing Maps (SOMs)

SOMs are a neural network technique which can plot the connections of input data on maps by their degree of similarity. Using this function, multidimensional data, which are generally difficult to comprehend, can be classified on two-dimensional maps, and can be clearly visualized (Kohonen, 1990, Vesanto, 2000).

Figure 4 shows the ordering of nodes on the SOM map. In the SOM algorithm, the patterns are trained based on input vector (the data to be classified) from the input layer. The arranged pattern on each node is described by the

Table 1. Distribution of observation wells and data used.

Site No.	Well No.	Difference in water level (a)	(b)	(c)	(d)	Strainer depth (e)	Site name
1	1	−12.5	−11.2	4.8	0.1	−72	Minamisuna
	2	−14.8	−7.8	3.9	−0.8	−132	
2	1	−14.0	−15.0	−0.1	2.2	−63	Kameido
	2	−27.3	−0.1	−0.4	1.4	−146	
3	1	−4.0	−13.1	6.9	2.9	−48	Azuma
	2	−40.4	21.1	7.5	23.3	−116	
4	1	6.1	−10.9	1.1	29.4	−35	Ryougoku
	2	−27.1	4.2	35.7	34.0	−85	
5	①	5.3	−9.7	−5.2	−14.9	−12	Shin-Edogawa
	2	−32.8	2.3	11.3	20.1	−152	
	3	−22.7	−5.3	3.9	3.2	−348	
6	1	10.4	91.1	19.2	−7.3	−52	Koiwa
7	1	−18.3	−14.4	11.1	8.9	−66	Edogawa - East
	2	−25.8	−2.4	8.4	16.1	−159	
	3	−20.0	−1.4	1.6	8.5	−305	
8	1	14.8	−13.5	−5.4	−7.0	−40	Kojima
	2	−83.3	7.5	30.1	7.1	−77	
	3	−38.2	5.4	27.0	10.2	−134	
	4	−35.3	−6.0	19.6	11.7	−229	
9	1	−28.1	4.0	3.5	16.5	−58	Shinozaki
	2	−39.1	−1.8	−1.0	4.4	−258	
	3	−24.4	−3.2	0.4	6.9	−313	
10	1	−30.4	0.2	11.8	35.4	−234	Shin-Adachi
11	1	−19.6	40.3	0.0	102.1	−112	Ikou
12	1	−32.4	7.3	7.6	43.4	−103	Shinmei -South
	2	−36.6	17.5	11.8	69.2	−176	
	3	−35.8	0.8	4.4	8.6	−329	
13	1	−2.1	−7.1	2.4	−1.3	−43	Odai
	2	−35.7	8.0	7.3	28.3	−158	
	3	−8.4	−20.5	−1.0	8.9	−232	
14	2	−32.7	15.9	5.3	144.7	−181	Toneri
	3	−24.1	10.8	5.2	12.2	−299	
	④	23.4	−22.0	−12.3	−14.2	−3	
15	1	−32.3	−0.6	−2.9	5.2	−122	Takasago
16	1	−27.9	−24.5	−5.4	−14.2	−265	Todabashi
	2	−24.0	12.2	−13.7	64.4	−110	
	3	−23.0	4.7	−6.5	55.4	−56	
17	1	−68.3	24.7	0.8	7.2	−170	Itabashi
18	1	−23.5	43.3	10.7	20.0	−95	Kami-Akatsuka
	2	−17.2	−11.1	−0.5	0.3	−184	
	3	−13.4	−10.1	−1.2	−8.4	−328	
19	1	−39.5	28.7	12.9	78.1	−55	Nerima
	2	−19.2	−3.6	1.9	51.2	−153	
20	1	−26.4	14.2	21.0	51.0	−92	Shinjyuku
21	1	−28.4	−0.6	24.4	39.2	−106	Suginami
	②	−0.6	−2.7	−4.7	−21.7	29	
22	1	−17.6	2.1	5.0	4.1	−68	Setagaya
23	1	−33.6	−10.0	−5.4	−38.0	−130	Meguro
	②	−14.4	−12.5	−4.4	−23.0	4	
24	1	−1.6	−0.8	3.2	−5.8	−13	Chiyoda
	2	−25.6	11.4	24.5	49.4	−94	
25	1	−24.9	37.2	−4.6	179.1	−50	Higashi-Kurume
	2	−24.6	18.0	1.4	130.8	−129	
	3	−25.1	−1.8	3.0	16.4	−377	
	④	−0.1	0.0	−0.4	−1.4	35	
26	1	−0.8	−6.7	9.5	−4.3	9	Choufu
	2	−28.2	14.7	25.5	309.6	−19	
	3	−15.1	26.2	45.5	411.0	−61	
	4	−19.8	3.2	22.3	285.3	−128	
27	1	−25.3	−5.4	−10.0	32.8	−29	Kiyose
	2	−42.3	17.6	0.9	81.6	−142	
	3	−18.1	−1.5	4.1	16.4	−373	
	④	−0.2	−1.1	−2.7	−8.6	35	
28	1	−20.0	8.4	7.6	14.5	16	Higashi-Yamato
	2	−54.8	3.7	9.2	177.0	−68	
	3	−21.1	−5.2	5.5	248.9	−151	
	④	0.4	−2.2	1.2	−1.2	86	
29	1	−34.6	31.8	19.5	99.3	−27	Tachikawa
	2	−19.0	0.8	17.0	98.6	−180	
	③	−0.2	−1.3	−5.0	−11.8	68	
30	1	−2.7	−1.7	15.1	42.1	−12	Koganei
	2	−19.6	−6.7	1.7	111.2	−80	
	3	−21.1	−3.6	8.5	115.4	−188	
31	1	−27.9	5.4	22.4	135.7	−78	Koganei -South
	2	−25.3	3.2	16.9	136.9	−142	
	③	−4.2	−4.6	−2.9	−9.4	39	
32	1	−18.3	−0.8	8.8	6.9	25	Musashi-Murayama
	2	−23.7	21.0	21.8	65.9	−50	
	3	−30.3	11.9	30.9	--	−140	
33	1	0.9	−4.5	1.5	−2.6	36	Fucyu
	2	−20.1	30.7	20.4	124.7	−84	
	3	−17.9	−6.6	3.0	--	−172	
34	1	−5.2	5.3	−2.5	−30.9	21	Higashi murayama
	2	−26.8	5.6	5.6	68.1	−118	
	3	−0.8	−24.1	7.7	71.7	−210	
35	1	−26.3	−28.3	−7.4	3.2	9	Hachiouji
	2	−18.3	−12.3	−9.3	−0.3	−66	
	③	0.2	0.3	0.9	4.1	99	
36	1	−22.5	4.5	18.0	38.4	49	Mizuho
	2	−24.8	30.0	11.2	52.1	−27	
37	②	−1.9	−1.2	−0.5	−1.8	40	Shin-Tama
38	1	−17.9	−1.6	14.5	101.9	−174	Inagi
41	1	−22.2	34.8	43.0	72.7	−57	Mitaka
	2	−23.2	8.4	26.4	223.9	−177	
	③	−0.4	−1.5	−1.7	−14.1	41	
42	1	−11.0	16.7	13.7	35.6	16	Akishima
	2	−16.0	−2.4	15.3	87.4	−91	
	③	0.5	4.3	6.8	20.9	106	

1) Well No. ○ ; Unconfined groundwater, 2) (a)～(d) ; cm,
3) (e) ; T.P.+ m, 4) -- ; Data missing,

multidimensional vector, called a reference vector, and each reference vector corresponds to one node. Reference vectors have the property of being similar to each other if they are closer, and being different if they are more distant on the SOMs (Jin et al., 2011).

The selection of input vectors by SOMs is trained so as to be organized according to Euclidean distances between input data. Therefore, it should be taken into consideration that the results of the SOM analysis are highly sensitive to the data pre-processing method used. The input data of the SOMs were standardized so that even a slight or long term water level change could be extracted from the raw data shown in Table 1.

Considering the diastrophism in Tokyo after the Great East Japan Earthquake was 4cm at the most, ± less than 5cm fluctuation water level in (a) to (d) is shown as 0, and ±5cm or any value greater is shown as +1 or -1 in this paper. Also, the depth of the strainers was input using the actual amount (in meters) of Tokyo Peil. The reference vectors are clustered on the map. In this paper, the most appropriate number of clusters is defined by the minimum DBI value (Davies-Bouldin Index) which applies *K*-means algorithm (Scott and Oyana, 2006; Jin et al., 2011; Nishiyama et al., 2007), and Ward's method is used for cluster classification. A heuristic rule of $m = 5\sqrt{n}$ is generally used to determine the SOM structure (Jin et al., 2011; Hentati et al., 2010; Hilario and Ivan, 2004). *m* denotes the total number of nodes and n is for the number of input data. Here, since *n* =98, the total number of nodes is 50, and a hexagonal array of 10 vertical nodes and 5 horizontal nodes was used, as shown in Fig. 4.

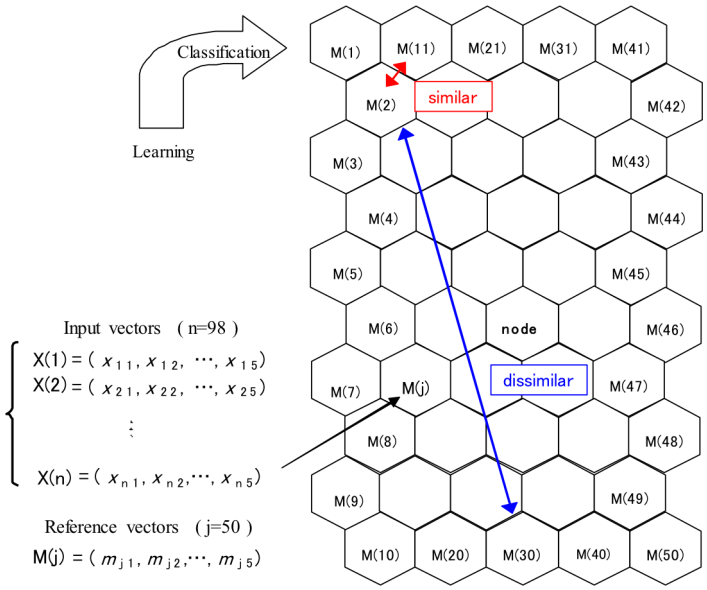

Figure 4. Component planes (10×5 nodes array).

3. Extraction of patterns from groundwater level fluctuation

Figure 5 shows the results of the reference vectors corresponding to the 5 items from (a) to (e) described earlier, using SOMs. (a) to (d) show the reference vectors standardized into [0, 1], and (e) shows the strainer depth of the reference vectors obtained. 50 nodes were classified into clusters by the techniques described earlier to understand the characteristics shown on Fig. 5 more easily. Figure 6 shows the change of DBI values corresponding to the number of clusters, and the lowest value is for 8 clusters. Figure 7 shows a dendrogram with node numbers classified into their 8 respective clusters.

In Figure 8, the arrangement of the 8 clusters is shown, as well as the number of observation wells in each node. In Figure 9, the number of each observation well from Table 1 is shown so that the characteristics of each well can be easily understood. Figure 10 shows the reference vectors of each cluster which are standardized into [0, 1] to understand the characteristics of the 8 clusters, and the first quartile, the median (i.e.,the second quartile), and the third quartile are plotted.

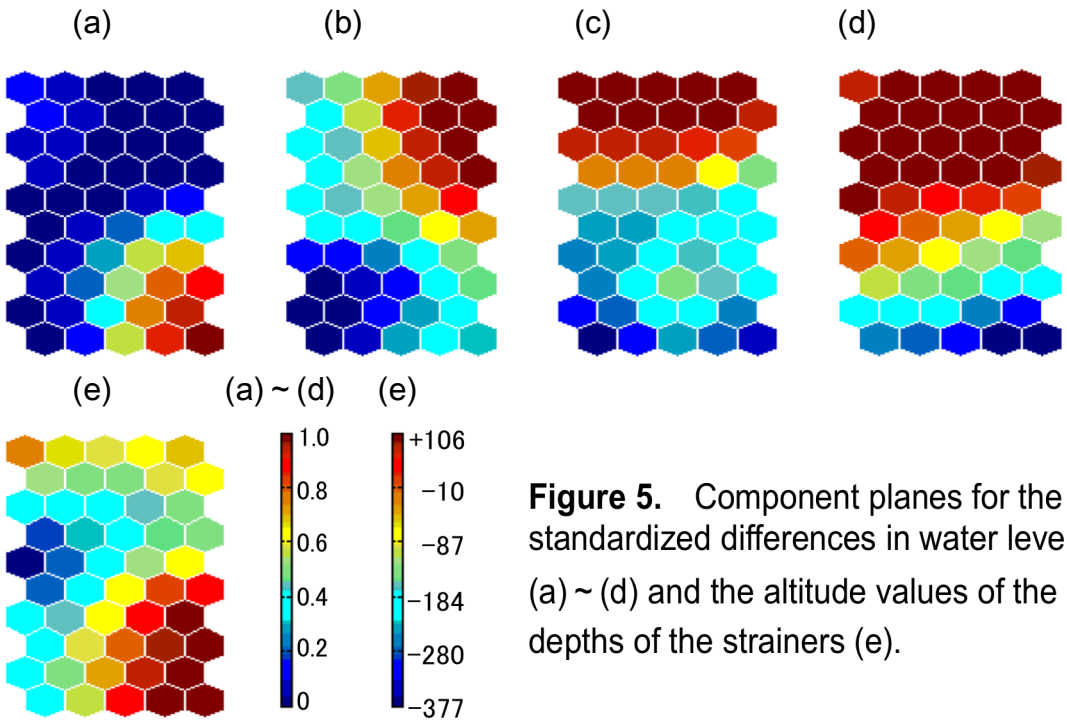

Figure 5. Component planes for the standardized differences in water levels (a) ~ (d) and the altitude values of the depths of the strainers (e).

Figure 6. Variation of DBI values with the optimal number of clusters.

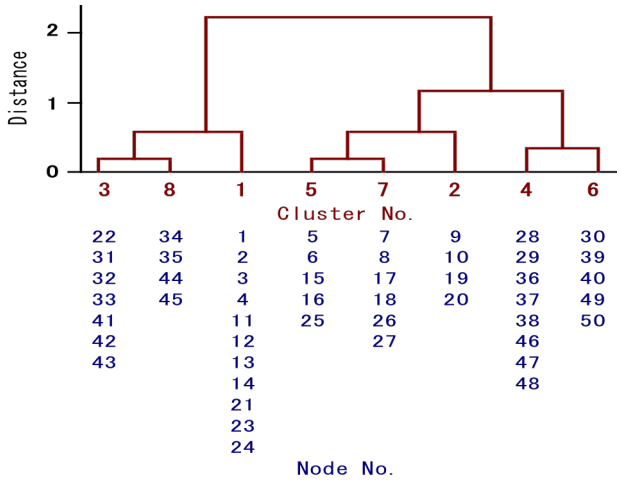

Figure 7. Dendrogram with node numbers classified into the respective clusters.

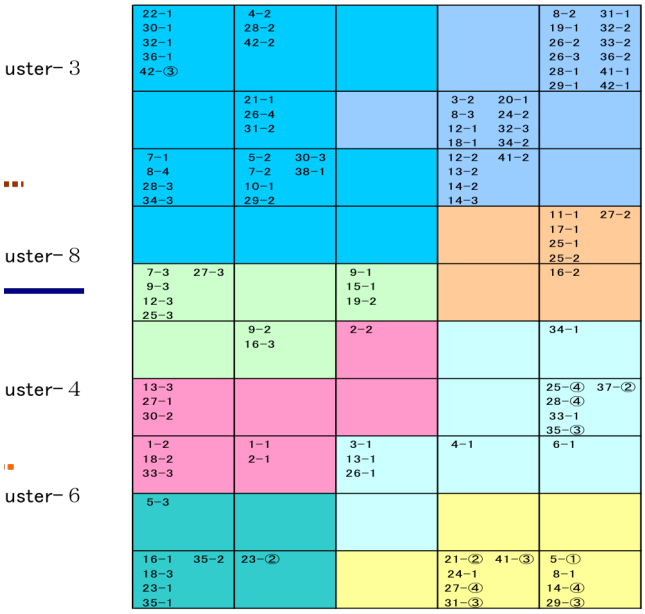

Figure 9. Index of observation wells classified into the respective nodes.

4. Pattern characteristics of water level fluctuation in each cluster

4.1 Pattern classification of water level fluctuation using SOMs

The characteristics of the distribution patterns in Fig. 5 and Fig. 8, and are shown as an overview, not focusing on the specific details of the distribution patterns, since standardized data are used in this analysis.

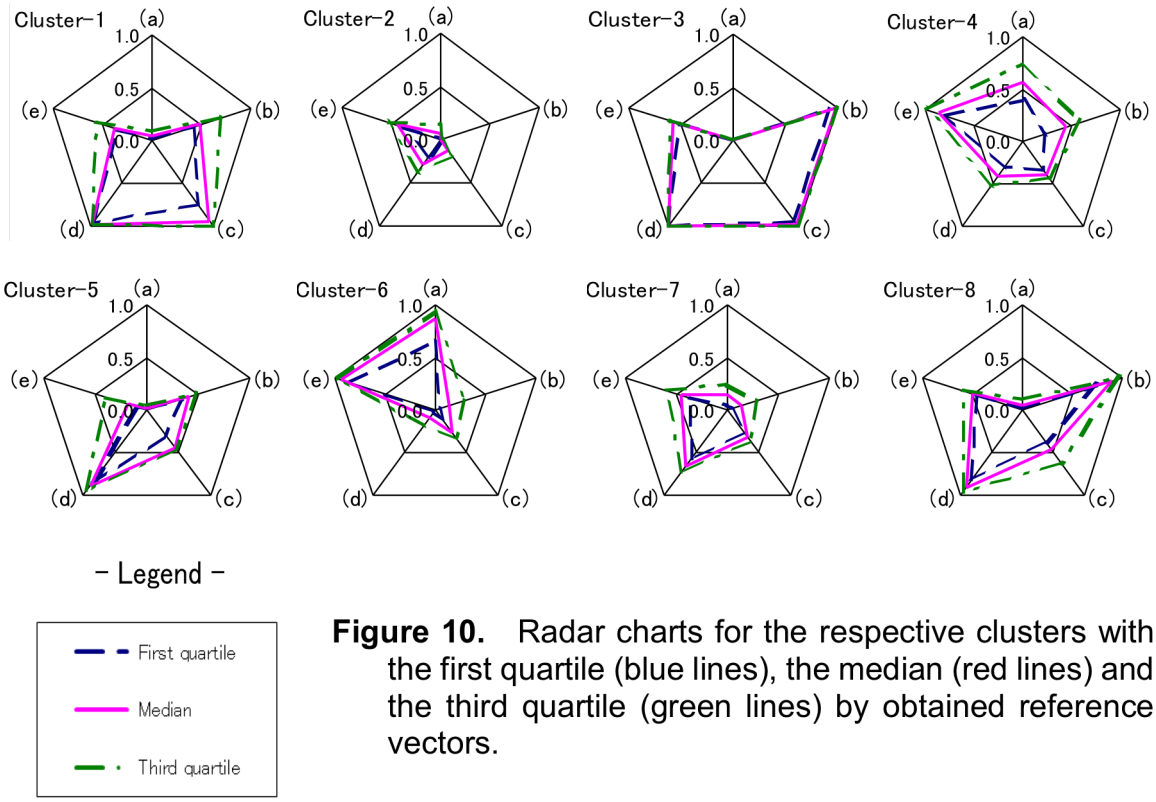

Figure 10. Radar charts for the respective clusters with the first quartile (blue lines), the median (red lines) and the third quartile (green lines) by obtained reference vectors.

As an overall characteristic in Fig. 5, the 4th line down from the top left, and the 5th line down from the top right of SOMs (a) to (d) divide them into upper and lower color patterns. The color patterns also show a clear difference in the left and right halves of each SOMs. The upper parts of the SOMs from (a) to (d) show a decreasing trend of the groundwater level, which then increases over time. (e) covers a broad range of wells, from deep to relatively shallow strainers. The clusters on the middle and lower left of Fig. 8 correspond to wells which have deep strainers, and show the increasing trend of groundwater level fluctuation after mid-March.

The clusters on the middle and lower right of Fig. 8 correspond to wells which have shallow strainers, and show the increasing trend of groundwater level fluctuation just after the earthquake.The main variability characteristics in each cluster are shown in Fig. 9 and Fig. 10.

In cluster 1, it can be seen that the groundwater level decreased significantly just after the earthquake, but by the following day, it had returned to the level just before the earthquake. It continued to increase until March 14 and remained at that level until March 31. The depth of the strainers is between (T.P.)-234 and +106 for these observation wells.

In cluster 2, it can be seen that the groundwater level decreased significantly just after the earthquake, and it remained at that level until the following day. By March 14, it had returned to the level slightly lower than just before the earthquake, and it kept recovering until March 31. The depth of the strainers is between (T.P.)-348 and +9.

In cluster 3, it can be seen that the groundwater level decreased the most in all the clusters at 16:00, March 11. It increased on the following day to a higher level than

just before the earthquake, and it remained at that level until March 31. The depth of the strainers is between (T.P.)-299 and +16.

In cluster 4, it can be seen that the groundwater level slightly increased or showed no significantly change just after the earthquake and from then on. The depth of the strainers is very between (T.P.)-52 and +99.

In cluster 5, it can be seen that the groundwater level decreased significantly just after the earthquake, and it had returned to the level just before the earthquake by the following day. It remained at this level until March 14, then continued increasing again until March 31. The depth of the strainers is between (T.P.)-377 and -56.

In cluster 6, no increase or drastic changes were observed just after the earthquake, and the groundwater level decreased on the following day to the level lower than just before the earthquake. It had returned to the level equivalent to just before the earthquake by March 14, and had fallen again by March 31. The depth of the strainers is between (T.P.)-40 and +68.

In cluster 7, the groundwater level shows a relatively significant decrease just after the earthquake, and it remained at that level until the following day. It returned to the level just before the earthquake on March 14, and continued increasing until March 31. The depth of the strainers is between (T.P.)-232 and -29.

In cluster 8, it can be seen that following the large decrease in groundwater level just after the earthquake, the level suddenly increase. It decreased again to the level just before the earthquake on March 14, and continued increasing until March 31. The depth of the strainers is slightly between (T.P.)-170 and -50.

4.2 Comparison between the results of visual time-series behaviors and those of SOMs

Regarding the fluctuation trend of the groundwater level, it has been shown in this paper that confined groundwater can be classified into 7 patterns, and unconfined groundwater can be classified into 3 patterns based on the visual time-series behaviors (hereafter called “subjective classification”) (Ishihara et al., 2012). The results of subjective classification and those of SOMs will be compared and examined below.

Table 2 shows the groundwater fluctuation patterns based on subjective classification, and their codes, characteristics and the number of wells. Table 3 shows the same codes and number of wells classified into 8 clusters using SOMs. In the subjective analyses, the confined and unconfined groundwater patterns were separately classified into 10 patterns in total, but in the SOM analyses, they were classified into 8 patterns without any distinction between confined and unconfined water levels.

Table 3. Results of SOM and subjective analyses.

SOMs Result		Classification patterns based on visual time-series behaviors in each cluster (Table-2)									
Cluster-No.	Num. of wells	Confined/Unconfined groundwater fluctuation patterns and number of wells									
Cluster- 1	21	C-D I	12	C-DR	5	C-DC	1	C-N	2	U-N	1
cluster- 3	25	C-D I	21	C-DR	3	C-DC	1				
cluster- 8	6	C-D I	5	C-DC	1						
cluster- 5	10	C-DC	5	C-DR	3	C-D I	2				
cluster- 7	9	C-DC	6	C-DI	2	C-DR	1				
cluster- 2	7	C-DC	6	U-D	1						
cluster- 4	11	U-N	4	C-N	4	C-I I	1	C-IC	1	C-DR	1
cluster- 6	9	U-N	5	U-I	2	C-N	1	C-ID	1		

In the subjective analyses, the patterns were classified using the water level changes just after the earthquake and on March 31. However, in the SOM analyses, the patterns were classified using standardized data and the depth of strainers. This caused the differences in the results in these two analyses. The Decresing trend patterns in confined groundwater level after the earthquake (C-D) in the subjective analyses were classified into 7 clusters in the SOM analyses. The Increasing trend patterns in unconfined groundwater level (U-I) in subjective analyses were classified into 1 cluster in the SOM analyses. The No significant change patterns (U-N, C-N) were classified into 3 clusters in the SOM analyses. There are a total of 8 clusters.

In Table 3, 2 to 5 of the fluctuation patterns from Table 2 are classified in each cluster. This appears to contradict the subjective classification trends, however, the main 2 patterns in each cluster in Table 3 represent as much as 73 to 100% of the patterns.

For example, 80% of the No significant change and Increasing trend patterns in unconfined observation wells in Table 2 are in Clusters 4 and 6 in Table 3. The

Table 2. Confined and unconfined groundwater fluctuation patterns based on subjective classification.

Confined		Groundwater level fluctuations	Wells
C-D	C-D I	**Confined groundwater** - **D**ecrease then **I**ncrease	42
	C-DC	**Confined groundwater** - **D**ecrease **C**ontinuing until end of March	20
	C-DR	**Confined groundwater** - **D**ecrease then **R**ecover to the level before the earthquake	13
C- I	C-I I	**C**onfined groundwater - **I**ncrease, temporary decrease, **I**ncrease again	1
	C-I C	**C**onfined groundwater - **I**ncrease **C**ontinuing until end of March	1
	C-I D	**C**onfined groundwater - **I**ncrease then **D**ecrease	1
C-N	C-N	**C**onfined groundwater - **N**o significant changes	7

Unconfined	Groundwater level fluctuations	Wells
U-D	**U**nconfined groundwater – **D**ecrease	1
U-I	**U**nconfined groundwater – **I**ncrease	2
U-N	**U**nconfined groundwater - **N**o significant changes	10

Increasing trend patterns just after the earthquake (C-I, U-I) showed Decreasing trends later, so these patterns were classified into the same clusters as the No significant change patterns (U-N, C-N), taking the overall fluctuation patterns and the depth of strainers into account. As of March 31, C-DR in Cluster 1 showed trends of water returning to their original levels after temporarily decreasing, and this is similar to the trends for C-DI, which showed water levels increasing after temporarily decreasing. Therefore, the results from the SOMs and from those of previous classifications can be considered as relatively the same.

Overall, the results of SOMs can be regarded as almost the same as those of subjective analyses taking into account the overall characteristics in Table 3 and Chart 8. It was clarified in this paper that SOMs enable objective and comprehensible pattern classifications to understand the characteristics of groundwater level fluctuations.

5. Conclusion

This paper categorized the fluctuation pattern characteristics of groundwater levels in the Tokyo area after the Great East Japan Earthquake using SOMs, a pattern classification technique. Five items were used as input data from 98 observation wells (85 confined and 13 unconfined) in 40 sites out of 42 groundwater level observation sites in the Tokyo Metropolitan area (excluding the islands and mountains of Tokyo). These 40 sites were used as they were less affected by blackouts. As a result, the fluctuation patterns of the groundwater level could be classified into 8 clusters.

It became clear in this paper that the trend of groundwater level fluctuation could be shown more objectively and comprehensibility using SOMs than subjective classification techniques. It also became clear that both techniques show almost the same results overall. Increases in groundwater level happen infrequently but it occurred at the time of the earthquake. Therefore, appropriately reflecting such increases was one of the issues with using SOMs.

In the SOM analyses, this increasing trend is classified into the same cluster as No significant change. This seems to be appropriate as it is an entirely different cluster from the main Decreasing trend cluster, and the observation wells with increasing trends right after the earthquake often showed decreasing trends later. It became clear that preprocessing from standardizing the input data is an important factor in showing clear characteristics. Therefore, using SOM analyses appears to be applicable in the field of groundwater observation.

We would like to further promote analyses of groundwater level fluctuation in Tokyo using SOMs in more multidimensional and complicated pattern analyses with long-term input data.

References

AIST-GSJ. (2011) Changes in groundwater and crustal strain in Tokai, Kinki and Shikoku related to the 2011 Off the Pacific Coast of Tohoku Earthquake (M9.0) :

Report on The Coordinating Committee for Earthquake Prediction. *Geological Survey of Japan, National Institute of Advanced Industrial Sceince and Technology,* No.300, 27-32. (in Japanese).

Hentati, A., Kawamura, A., Amaguchi, H. and Iseri, Y. (2010) Evaluation of sedimentation vulnerability at small hillside reservoirs in the semi-arid region of Tunisia using the Self-Organizing Map : *Geomorphology*, 122, 56-64.

Hilario, L.G. and Ivan, M.G. (2004) Self-organizing map and clustering for wastewater treatment monitoring : *Engineering Applications of Artifical Intelligence,* 17, 215-225.

Iseri, Y., Mizumoto, M., Jinno, K. and Nishiyama, K. (2009), Use of the Self-Organizing Maps for the investigation of variability characteristics of monthly precipitation distribution across the Japan : *J. Jpan Soc. Hydrol. and Water Resour,* 22(6), 466-478. (in Japanese).

Iseri, Y., Nishiyama, K., Jinno, K. and Kawamura, A. (2010) Pattern extraction of 500 hpa daily temperature field surrounding Japn using various pattern recognition methods. : *Hydraulic Engineering Journal of Society of Civil Engineers*, 54, 439-444. (in Japanese).

Iseri, Y. and Kagari, S. (2013) Exatration of track and intensity patterns from historical tropical cyclones using the self-organizing map. : *J. Jpn. Soc. Civ. Eng. Ser. G,* 69 (5), I_61-I_66. (in Japanese).

Ishihara, S., Kawamura, A., Amaguchi, H., Takasaki, T. and Kawai, M. (2012) Characteristics of unconfined and confined groundater level fluctuation inTokyo by the 2011 Off the pacific Coast of Tohoku Earthquake. : *J. Jpn. Soc. Civ. Eng. Ser. B1,* 68 (4), I_595-I_600. (in Japanese).

Itadera, K., Kikugawa, J. and Daita, Y. (2011) Changes in temperature and discharge of hot spring waters observed in Hakone spas caused by the 2011 off the Pacific coast of Tohoku Earthquake : *Report on Hot Springs Research Institute of Kanagawa Prefecture*, 43, 39-43. (in Japanese).

Jin, Y.H., Kawamura, A., Park, S.C., Nakagawa, N., Amaguchi, H. and Olsson, J. (2011) spatiotemporea, using self-orgaizing maps : *J Environ. Monit.,* 13, 2886-2894.

JMA. (2012) Report on the 2011 Off the Pacific Coast of Tohoku Earthquake by Japan Meteorogical Agency : *Technical report of the Japan Meteorogical Agency*.

Kagawa, J., Furuno, K. and Yamamoto, M. (2013) Groundwater level change due to the effect of earthquake in Chiba Prefecture : *2013 Annual report on Research Institute of Enviromental Geology. Chiba Prefecture,* Available from http://www.pref.chiba.lg.jp/wit/chishitsu/nenpou/npchishitsu.html [Accessed 19th November 2014]. (in Japanese).

Kawai, M., kawashima, S., Ishihara, S. and Takahashi, K. (2012) Characteristics of groundwater level variation in 2011 : *2012 Annual report on Civil Engineering and Trainig Center, Tokyo Metropolitan Government*, 131-150. (in Japanese).

Kitagawa, Y. and Koizumi, N. (2011) Changes in groundwater levels, groundwater pressures and discharge rates a day after the 2011 Off the Pacific Coast of Tohoku Earthquake(M9.0) : *Report on Active Fault and Paleoearthquake Researches, AIST-GSJ*, 11, 309-318. (in Japanese).

Kohonen, T. (1990) The Self-Organizing Map. : *Proceedings of The IEEE*, 78(9), 1464-1480.

Kokubun, K. and Tsuchiya, M. (2003), Charateristics of groundwater recharge and Hydrologic Cycle at Musashino Plateau in Tokyo : *J. Jpan Soc. Hydrol. and Water Resour.,* 16(3), 289-300. (in Japanese).

Nguyen, T.T., Kawamura, A., Tong, N.T., Nakagawa, N. and Amaguchi, H. (2015) Clustring spatio-seasonal hydrogeochemical data using self-organizing maps for groundwater quality assessment in the Red River Dleta : *Journal of Hydrology*, 522, 661-673.

Nguyen, T.T., Kawamura, A., Tong, N.T., Amaguchi, H. Nakagawa, N. Gilbuena Jr.R. and Bui, D.D. (2015) Identification of spatio-seasonal hydrogeochemical characteristics of the unconfined groundwater in the Red River Dleta, Vietnam : *Applied Geochemistry*, 63, 10-21.

Nishiyama, K., Endo, S., Jinno, K. and Kawamura, A. (2005) Classification of meteorolical fields characterized by Baiu season using Self-organizing map. : *Hydraulic Engineering Journal of Society of Civil Engineers*, 49, 241-246. (in Japanese).

Nishiyama, K., Endo, S., Jinno, K. and Uvo, C.B., Olsson, J. and Berndtsson, R. (2007) Identification of typical synoptic patterns causing heavy rainfall in the rainy season in Japan by a self-organizing map. : *Atoms. Res.,* 83, 185-200.

Scott, K.E. and Oyana, T.J. (2006) An improved algorithm for segregating large geospatial data : *9th Agile Corfernence on Geographic Infomation Scirence*, 177-185.

TMG (1979) Study on the Fluctuation of groundwater level caused by earthquakes : *Surveillance study Report on Earthquake Division, Tokyo Disaster Prevention Conference, Tokyo Metropolitan Government*. (in Japanese).

TMG-BE. (2011) Re-verification of Land Subsidence and Groundwater of Tokyo Metropolis : *Report on 2011 Committee of Grounwater Measurement*. *Bureau of Environment, Tokyo Metropolitan Government*. (in Japanese).

TMG-CETC (2011) Land subsidence due to groundwater withdrawal, 2010 : *2011 Annual report on Civil Engineering and Trainig Center, Tokyo Metropolitan Government*, 163-188. (in Japanese).

Tokyo Electric Company. (2011) *Implementation of rolling blackout and request for further energy saving, 13rd Mar, 2011*. : Available from http://www.tepco.co.jp/en/press/corp-com/release/11031313-e.html [Accessed 3rd December 2015].

Vesanto, J., Himberg, J., Alhoniemi, E. and Parahankangas, J. (2000) SOM Toolbox for matlab 5. : *Helsinki University Report A57*.